

**SHOCK DEVOLATILIZATION OF CI CHONDRITE SIMULANTS.** K. Kurosawa<sup>1</sup>, R. Moriwaki<sup>1</sup>, H. Yabuta<sup>2</sup>, K. Ishibashi<sup>1</sup>, G. Komatsu<sup>3,1</sup>, and T. Matsui<sup>1</sup>, <sup>1</sup>Planetary Exploration Research Center, Chiba Institute of Technology (2-17-1, Tsudanuma, Narashino, Chiba 275-0016, Japan, [kosuke.kurosawa@perc.it-chiba.ac.jp](mailto:kosuke.kurosawa@perc.it-chiba.ac.jp)), <sup>2</sup>Dept. Earth and Planet. Sys. Sci., Hiroshima Univ., Japan. <sup>3</sup>Int. Res. Sch. of Planet. Sci., Università d'Annunzio, Italy

**Introduction:** C-type asteroids has been thought to be parent bodies of carbonaceous chondrites, which include a plenty of water (6–20 wt%) and carbon (~3 wt%) [e.g., 1]. Thus, it has been widely considered that C-type asteroids are among the main carrier of water and organics into the inner Solar System [e.g., 2].

Recently, two C-type asteroids, Ryugu and Bennu, have been extensively explored by Hayabusa2 [e.g., 3] and OSIRIS-REx [e.g., 4], respectively. The remote-sensing observations reveal that Ryugu and Bennu have suffered a number of impacts with a variety of impact energies [e.g., 5]. Shock features in recovered samples will be identified and investigated extensively by mineralogical, petrological, and chemical analyses. To maximize the scientific results from the returned samples, the knowledge about responses of C-type asteroid-like materials against impact shocks is necessary.

In this study, we conducted hypervelocity impact experiments using a simulant of CI carbonaceous chondrite [6] as an analog of the constituent materials of C-type asteroids. We measured the amount and the composition of shock-generated gas from the analog.

**Experiments:** The impact experiments were conducted using a two-stage light gas gun placed at the hypervelocity impact facility of Planetary Exploration Research Center of Chiba Institute of Technology (PERC/Chitech), Japan [7].

**Experimental conditions:** We made pellets 54 mm in diameter and ~30 mm in thickness from the CI simulant provided by Exolith (<https://sciences.ucf.edu/class/exolithlab/>). The bulk density of the pellets is  $1.91 \pm 0.04$  g/cm<sup>3</sup>, which is close to the typical density of carbonaceous chondrites. The porosity is estimated to be ~25% based on the grain density of Orgueil chondrites [6]. In order to investigate the devolatilization behavior of the CI simulant, we used the two-valve method developed by [8]. The method allows us to measure shock-generated gas in an open system, which is the same geometry of natural impact phenomena, with a small risk of chemical contamination from the gun operation. In addition, we used He gas instead of usually-used H<sub>2</sub> gas for projectile acceleration to exclude the possibility that the trace amount of H<sub>2</sub> gas intruded into the experimental chamber contributes to chemical reduction. A quadrupole mass spectrometer (QMS, Pfeiffer vacuum, Prisma plus QMG220) was used to measure the shock-generated gas after each impact. An Al<sub>2</sub>O<sub>3</sub> sphere 2 mm in diameter ( $D_p = 2$  mm) was used as a projectile and was accelerated using a

nylon-slit sabot [9]. In this study, we conducted three shots (#440, #447, and #448) at nearly-identical impact velocities  $v_{\text{imp}} = 5.8 - 5.9$  km/s.

**Calibration:** We also conducted a series of calibration experiments by using a gas injection device and gas mixtures with different mixing ratios of CO<sub>2</sub> to Ar because CO<sub>2</sub> was the dominant detected gas in all the shots. A gas mixture between Ar and CO<sub>2</sub> was injected into the experimental chamber with a short duration (~0.1 s) using an automatic gate valve.

**Numerical simulations:** Experienced pressure and temperature in the target were estimated by the iSALE-2D [10-12]. The Tillotson EOS [13] for Al<sub>2</sub>O<sub>3</sub> and the ANEOS [14] for serpentine [15] were employed for projectile and target, respectively. Serpentine is the main constituent of the CI simulant. The  $\epsilon$ - $\alpha$  porosity compaction model [12] was used to treat the porous target. The projectile was divided into 50 cells per projectile radius. The expected residual temperature of each tracer particle was estimated by the entropy. The impact velocity was set to the same achieved in the experiments.

**Results:** Figure 1 shows the time variations of the ion currents of selected mass numbers at shot #448. The ion current for the mass number  $M/Z = i$  is denoted as  $I_i$ . We confirmed that  $I_{40}(\text{Ar}^+)$  is stable during the measurement. The rise in  $I_4(\text{He}^+)$ , which is the driver gas of the projectile, was not detected, suggesting that we successfully excluded the chemical contamination due to the gun operation from the gas-phase chemical analysis. We detected sudden rises in  $I_2(\text{H}_2^+)$ ,  $I_{16}(\text{CH}_4^+)$ ,  $I_{28}(\text{CO}^+)$ ,  $I_{44}(\text{CO}_2^+)$ , and  $I_{34}(\text{H}_2\text{S}^+)$ , but did not detected the rise in  $I_{18}(\text{H}_2\text{O}^+)$ . The contributions of the cracking of heavier species due to electron impacts in the QMS to the ion currents for lighter species were investigated using standard gases. For example, a certain fraction of CO<sub>2</sub> is decomposed into CO and O in the QMS measurement. We extracted such the contributions in  $I_i$  from the raw signals by using the cracking patterns obtained by the standard gases of CH<sub>4</sub>, H<sub>2</sub>O, CO, and CO<sub>2</sub>.

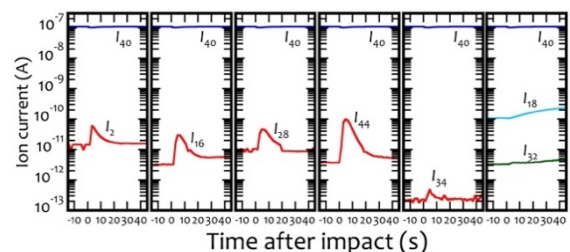


**Figure 1.** The time variations of the ion currents of the selected chemical species at Shot #448.

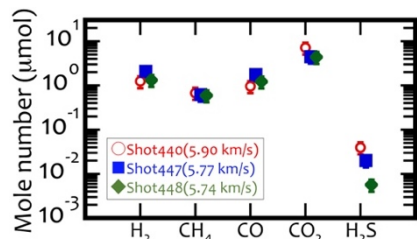


**Figure 2.** The produced mole number. The error is  $\pm 30\%$  and is come from the calibration experiments.

We measured the produced mole number of the detected species quantitatively by integrating the time profile of the ion currents and by assuming the ratio of the integrated values for the species except for  $\text{CO}_2$  to that for  $\text{CO}_2$  is linearly proportional to the molar ratios to  $\text{CO}_2$ . Figure 2 shows the produced mole numbers of  $\text{H}_2$ ,  $\text{CH}_4$ ,  $\text{CO}$ ,  $\text{CO}_2$ , and  $\text{H}_2\text{S}$ . The main product was  $\text{CO}_2$  at all the shots. The mass of the  $\text{CO}_2$  production corresponds to 1–2 wt% of the projectile mass  $M_p$ . The amounts of the reducing species ( $\text{H}_2$ ,  $\text{CH}_2$ , and  $\text{CO}$ ) were 10–50 mol% of the  $\text{CO}_2$  produced. We found that the amount of S-bearing gases was only 0.1–0.01 mol% of C-bearing gases although the sulfur content in the CI simulant is similar to the carbon one. We also found that the water loss from hydrous minerals, which are the main constituents of the CI simulant, was not significant. The upper bound of the released mole number of water vapor was roughly estimated to be 1.1-fold  $\text{CO}_2$  mole number at shot #448 using the ratio of  $I_{18}$  to the peak value of  $I_{44}$ .

**Discussion & Conclusions:** The peak pressure at the impact point was estimated to be 65 GPa by the iSALE-2D. The corresponding  $v_{\text{imp}}$  of the collision between two porous serpentine was 8.5 km/s, which is higher than the typical  $v_{\text{imp}}$  in the main belt region ( $\sim 5$  km/s [16]). Figure 3a shows a snap shot and a provenance plot of the numerical results for shot #448 at  $t = 3 t_s$ , where  $t$  is time after impact,  $t_s = D_p/v_{\text{imp}}$  is the characteristic time for projectile penetration. The color indicates the expected residual temperature  $T_{\text{res}}$  at the time estimated by temporal entropy. Figure 3b shows the cumulative mass experienced a  $T_{\text{res}}$  higher than the given  $T_{\text{res}}$ . According to a thermal decomposition experiment using the CI simulant, the temperature required for incipient volatile release except for desorbed water is  $\sim 800$  K [6]. The mass of the heated target with  $T_{\text{res}} > 800$  K is  $\sim 4 M_p$ . Since the total volatile content of the CI simulant is  $\sim 10$  wt% [6], the upper limit of the volatile release is estimated to be  $\sim 40$  wt% of  $M_p$ . In contrast, the actual released amount was only a few wt% of  $M_p$ , which is  $\sim 1/10$  of the upper limit, indicating that the heated volume was thermally buffered due to the latent heat of the thermal decomposition of the organics contained in the CI simulant. This may be the reason why

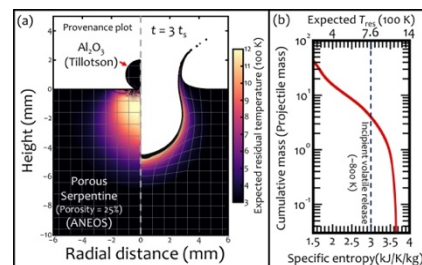


**Figure 3.** (a) a provenance plot and a snap shot at  $t = 3 t_s$ . (b) The cumulative mass as a function of specific entropy. The expected residual temperature estimated by the entropy is also shown as the top X-axis.

the water loss is highly limited even though the CI simulant is mainly composed of hydrous minerals ( $\sim 50$  wt%). The stability of the hydrous minerals in the CI simulant (mainly Mg-serpentine) against a high temperature is higher than the organics (mainly coal) [6].

If the CI simulant is a good analog of the constituent materials of C-type asteroids, our results are useful to predict the response of the C-type asteroids against impact shocks as follows.

(1) The impact-induced volatile release is limited only to 1–2 wt% of the impactor mass even at a relatively high-speed collision in the main belt (8.5 km/s).

(2) The water loss due to impact shocks is not significant because post-shock temperature field is thermally buffered by the decomposition of insoluble organic matters (IOM).

(3) The devolatilization of S-bearing minerals at the typical collision in the main belt region is unlikely.

**Acknowledgments:** This work was supported by ISAS/JAXA as a collaborative program with the Hypervelocity Impact Facility. We appreciate the developers of iSALE, including G. Collins, K. Wünnemann, B. Ivanov, J. Melosh, and D. Elbeshausen. We also thank Tom Davison for the development of the pySALEPlot.

**References:** [1] Baker, B. L. (1971) *Space Life Sciences*, 2, 472-497. [2] Hayatsu, R. & Anders, E. (1981) *Top. Curr. Chem.*, **99**, 1c-37. [3] Watanabe, S. et al. (2019), *Science*, **364**, eaav8032. [4] Lauretta, D. S. et al. (2019), *Nature*, **568**, 55-60. [5] Sugita, S. et al. (2019), *Science*, **364**, eaaw0422. [6] Britt, D. T. et al. (2019), *MAPS*, **54**, 2067-2082. [7] Kurosawa, K. et al. (2015) *JGR*, **120**, 1237-1251. [8] Kurosawa, K. et al. (2019), *GRL*, **46**, 7258-7267. [9] Kawai N. et al. (2010) *RSI*, **81**, 115105. [10] Amsden A. A., et al. (1980) *LANL Report LA-8095*. 101 p. [11] Ivanov B. A., et al. (1997), *IJIE*, 20, 411. [12] Wünnemann, K., et al. (2006), *Icarus*, 180, 514. [13] Tillotson, J. H. (1962). *Tech. Rep. GA-3216*, General Atomic Report. [14] Thompson, S. & Lauson, H. (1972), *SNL Rep.*, SC-RR-71 0714:113p. [15] Brookshaw, L. (1998), *Tech. Rep.*, SC-MC-9813. [16] Bottke, W. F. et al. (1994), *Icarus*, **107**, 255-268.